On the non-local geometry of turbulence

I. Bermejo-Moreno and D. I. Pullin

Small-scale turbulence;
Theory, phenomenology and Applications

Cargèse, August 13-25, 2007

Previous work

Different identification criteria for structures in turbulence exist.

Two main groups:

- based on the velocity gradient tensor and related quantities:
  - Λ (Chong),
  - Q (Hunt),
  - λ_2 (Jeong and Hussain),
  - $\lambda_{+,-}$(Horiuti).
- based on the pressure field: sectionally minimal pressure (Kida).

Previous work

Different identification criteria for structures in turbulence exist.

Two main groups:

- based on the velocity gradient tensor and related quantities:
  - Λ (Chong),
  - Q (Hunt),
  - λ_2 (Jeong and Hussain),
  - $\lambda_{+,-}$(Horiuti).
- based on the pressure field: sectionally minimal pressure (Kida).

Usually, two main types of structures considered: tubes and sheets.

Previous work

Different identification criteria for structures in turbulence exist.

Two main groups:

- based on the velocity gradient tensor and related quantities:
  - Λ (Chong),
  - Q (Hunt),
  - λ_2 (Jeong and Hussain),
  - $\lambda_{+,-}$(Horiuti).
- based on the pressure field: sectionally minimal pressure (Kida).

Usually, two main types of structures considered: tubes and sheets.

Most of these methods are local (point-wise criteria).

Previous work

Different identification criteria for structures in turbulence exist.

Two main groups:

- based on the velocity gradient tensor and related quantities:
  - Λ (Chong),
  - Q (Hunt),
  - λ_2 (Jeong and Hussain),
  - $\lambda_{+,-}$(Horiuti).
- based on the pressure field: sectionally minimal pressure (Kida).

Usually, two main types of structures considered: tubes and sheets.

Most of these methods are local (point-wise criteria).

Multi-scale analysis previously used in turbulence (e.g. Coherent Vortex Simulation, developed by Farge and Schneider).

Extraction

Purpose: educe structures associated to different ranges of scales.

Extraction

Purpose: educe structures associated to different ranges of scales.

Ranges of scales generally defined in Fourier space.

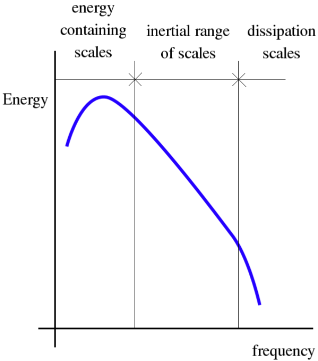

Extraction

Purpose: educe structures associated to different ranges of scales.

Ranges of scales generally defined in Fourier space.

But Fourier-basis functions are not localized in physical space.

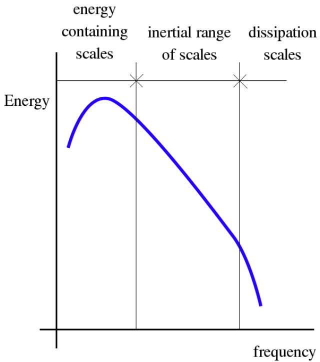

Extraction

Purpose: educe structures associated to different ranges of scales.

Ranges of scales generally defined in Fourier space.

But Fourier-basis functions are not localized in physical space.

$\Rightarrow$ Top-hat window filtering inappropriate.

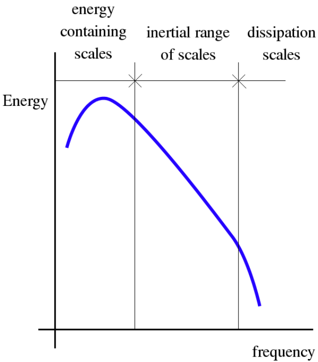

Extraction

Purpose: educe structures associated to different ranges of scales.

Ranges of scales generally defined in Fourier space.

But Fourier-basis functions are not localized in physical space.

$\Rightarrow$ Top-hat window filtering inappropriate.

Use **curvelet transform** (Càndes et al.).

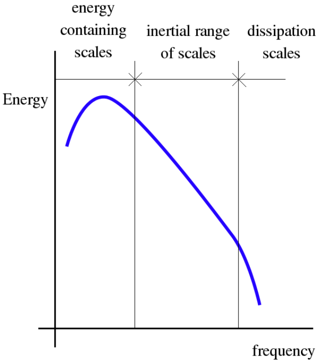

Curvelet transform

Curvelets are localized in scale (Fourier space), position (physical space) and orientation (unlike wavelets).

Curvelet transform

Curvelets are localized in scale (Fourier space), position (physical space) and orientation (unlike wavelets).
In Fourier space, they are defined by:

$$\hat{\varphi}^{D}_{j,l,k}(\omega) \equiv \tilde{W}_j(\omega)\,\tilde{V}_{j,\ell}(\omega)\exp\left(\frac{-2\pi i\sum_{i=1}^{3}\frac{k_i\omega_i}{L_{i,j,\ell}}}{\sqrt{\prod_{i=1}^{3}L_{i,j,\ell}}}\right)$$

Curvelet transform

Curvelets are localized in scale (Fourier space), position (physical space) and orientation (unlike wavelets).
In Fourier space, they are defined by:

$$\hat{\varphi}^{D}_{j,l,k}(\omega) \equiv \tilde{W}_j(\omega)\,\tilde{V}_{j,\ell}(\omega)\exp\left(\frac{-2\pi i\sum_{i=1}^{3}\frac{k_i\omega_i}{L_{i,j,\ell}}}{\sqrt{\prod_{i=1}^{3}L_{i,j,\ell}}}\right)$$

Radial and angular frequency windows satisfy:

$$\sum_{j\geq j_0}\tilde{W}_j^2(\omega)=1,\ \sum_{\ell=-\infty}^{\infty}\tilde{V}^2(t-2\ell)=1$$

j scale, ℓ orientation

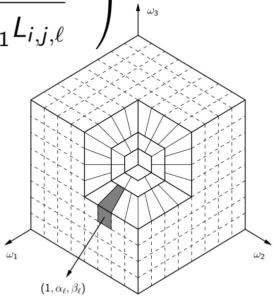

Curvelet transform

Properties

Curvelet transform

Properties

- Curvelets form a tight-frame in $L^2\left(\mathbb{R}^3\right)$.

Curvelet transform

Properties

- Curvelets form a tight-frame in $L^2(\mathbb{R}^3)$.
  Any function $f \in L^2(\mathbb{R}^3)$ can be expanded in a series of curvelets
  $$f = \sum_{j,\ell,k} \langle \phi_{j,\ell,k}, f \rangle \phi_{j,\ell,k}$$
  being $\phi_{j,\ell,k}$ the curvelet at scale j, orientation ℓ and position $k = (k_1, k_2, k_3)$.
  Parseval's identity holds: $\sum_{j,\ell,k} \|\langle f, \phi_{j,\ell,k} \rangle\|^2 = \|f\|^2_{L^2(\mathbb{R}^3)}$

Curvelet transform

Properties

- Curvelets form a tight-frame in $L^2\left(\mathbb{R}^3\right)$.
  Any function $f \in L^2\left(\mathbb{R}^3\right)$ can be expanded in a series of curvelets
  $$f = \sum_{j,\ell,k} \langle \phi_{j,\ell,k}, f \rangle \phi_{j,\ell,k}$$
  being $\phi_{j,\ell,k}$ the curvelet at scale j, orientation ℓ and position $k = (k_1, k_2, k_3)$.
  Parseval's identity holds: $\sum_{j,\ell,k} \|\langle f, \phi_{j,\ell,k} \rangle\|^2 = \|f\|^2_{L^2(\mathbb{R}^3)}$
- *Parabolic scaling*: in physical space width≈length^2

Curvelet transform

Properties

- Curvelets form a tight-frame in $L^2\left(\mathbb{R}^3\right)$.
  Any function $f \in L^2\left(\mathbb{R}^3\right)$ can be expanded in a series of curvelets
  $$f = \sum_{j,\ell,k} \langle \phi_{j,\ell,k}, f \rangle \phi_{j,\ell,k}$$
  being $\phi_{j,\ell,k}$ the curvelet at scale j, orientation ℓ and position $k = (k_1, k_2, k_3)$.
  Parseval's identity holds: $\sum_{j,\ell,k} \|\langle f, \phi_{j,\ell,k}\rangle\|^2 = \|f\|^2_{L^2(\mathbb{R}^3)}$
- *Parabolic scaling*: in physical space width≈length^2
- Curvelets are an optimal (sparse) basis for representing surface-like singularities of codimension one.

Iso-contouring

After the multi-scale decomposition, a set of fields associated to each range of scales results.

Iso-contouring

After the multi-scale decomposition, a set of fields associated to each range of scales results.

Iso-contours of each field corresponding to equivalent contour values (e.g. mean plus certain times the r.m.s.) are educed.

Iso-contouring

After the multi-scale decomposition, a set of fields associated to each range of scales results.

Iso-contours of each field corresponding to equivalent contour values (e.g. mean plus certain times the r.m.s.) are educed.

Periodic reconnection: structures intersecting periodic boundaries are reconnected to their continuation on the opposite boundary.

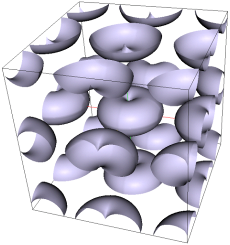

$\longrightarrow$

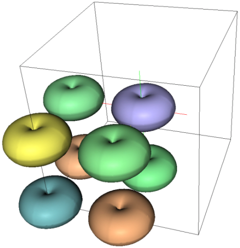

Characterization

Purpose: geometrically characterize structures based on their global shape.

Characterization

Purpose: geometrically characterize structures based on their global shape.

A two-step method is used:

Characterization

Purpose: geometrically characterize structures based on their global shape.

A two-step method is used:

1. A suitable set of differential geometry properties is locally obtained.

Characterization

Purpose: geometrically characterize structures based on their global shape.

A two-step method is used:

1. A suitable set of differential geometry properties is locally obtained.
2. Area-based probability density functions of those local properties are calculated (transition from local to global, in the surface sense).

Differential geometry properties

Shape index, Υ, and curvedness, Λ, (Koenderink) are the differential geometry properties chosen to represent locally the geometry of the surface.

Differential geometry properties

Shape index, Υ, and curvedness, Λ, (Koenderink) are the differential geometry properties chosen to represent locally the geometry of the surface.

They are related to the *principal curvatures* κ_1, κ_2 by:

$$\Upsilon \equiv -\frac{2}{\pi} \arctan\left(\frac{\kappa_1 + \kappa_2}{\kappa_1 - \kappa_2}\right)$$

$$\Lambda \equiv \sqrt{\frac{\kappa_1^2 + \kappa_2^2}{2}}$$

Shape index is dimensionless.
Curvedness is dimensional (L^{-1}).

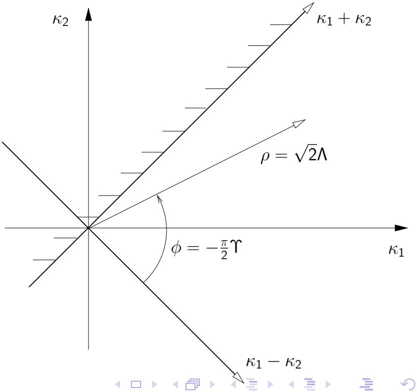

Shape Index

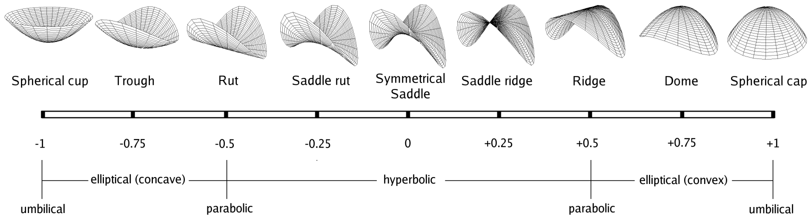

- Its absolute value $S \equiv |\Upsilon|$ represents the local shape of the surface at the point P, with $0 \leq S \leq 1$.

Shape Index

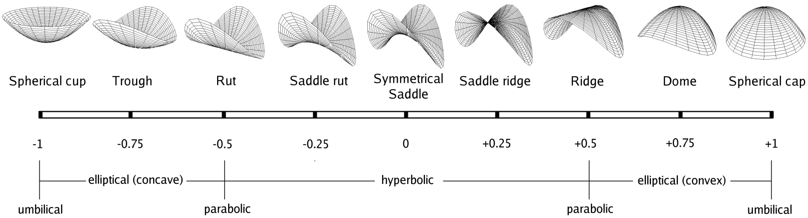

- Its absolute value $S \equiv |\Upsilon|$ represents the local shape of the surface at the point P, with $0 \leq S \leq 1$.
- Its sign indicates the direction of the normal, distinguishing, for example, convex from concave elliptical points.

Curvedness and stretching parameter

A nondimensionalization of Λ is required to compare the global shape of surfaces of different sizes:

$$C \equiv \mu\Lambda, \qquad \mu \equiv \frac{3\,V}{A}.$$

$V \equiv$ Volume[b], $A \equiv$ Area

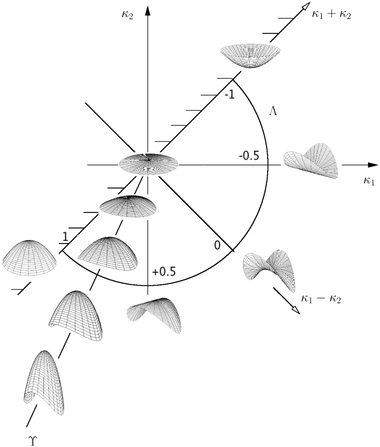

[b] Volume implies closed surface

Curvedness and stretching parameter

A nondimensionalization of Λ is required to compare the global shape of surfaces of different sizes:

$$C \equiv \mu\Lambda, \qquad \mu \equiv \frac{3\,V}{A}.$$

$V \equiv$ Volume[b], $A \equiv$ Area

Stretching parameter (global)

$$\lambda \equiv \sqrt[3]{36\pi}\,\frac{V^{2/3}}{A}$$

Example: $C_{sphere} = \lambda_{sphere} = 1$

[b]Volume implies closed surface

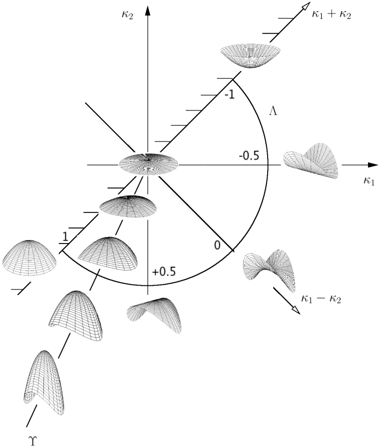

Signature of a structure

The area-based joint pdf $\mathcal{P}(S, C)$ † represents how the local shape, S, is distributed across the different (relative) scales, C.

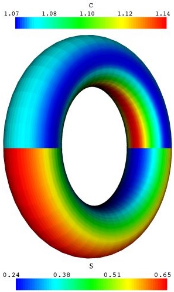

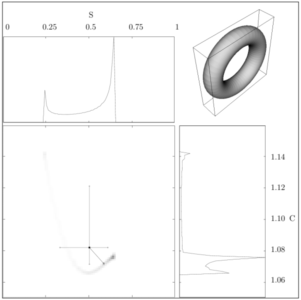

From $\mathcal{P}(S, C)$, marginal pdfs, $\mathcal{P}_{\mathcal{S}}(S)$, $\mathcal{P}_{\mathcal{C}}(C)$ can be obtained.

† $\int \int \mathcal{P}(S, C)\, dSdC = 1$

Signature of a structure

The area-based joint pdf $\mathcal{P}(S, C)$ † represents how the local shape, S, is distributed across the different (relative) scales, C.

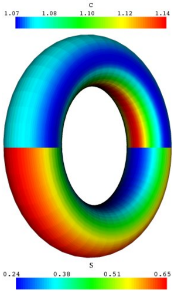

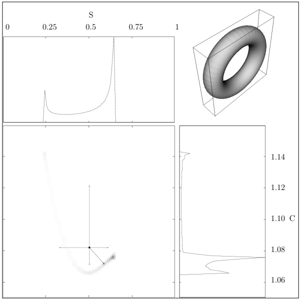

From $\mathcal{P}(S, C)$, marginal pdfs, $\mathcal{P}_\mathcal{S}(S)$, $\mathcal{P}_\mathcal{C}(C)$ can be obtained.

$\{\mathcal{P}(S, C), \mathcal{P}_\mathcal{S}(S), \mathcal{P}_\mathcal{C}(C), \lambda\}$ comprise the signature of a structure.

† $\int\int \mathcal{P}(S, C)\, dSdC = 1$

Classification

Purpose: assign structures to different groups, based on their signatures.

Classification

Purpose: assign structures to different groups, based on their signatures.

Learning-based clustering techniques are used.

Classification

Purpose: assign structures to different groups, based on their signatures.

Learning-based clustering techniques are used.

Properties:

- Locally-scaled
- Spectral
- K-means based
- Automatic determination of optimum number of clusters

Clustering algorithm

1. Start from N elements $E = \{e_1, \ldots, e_N\}$ and their signatures.

Clustering algorithm

1. Start from N elements $E = \{e_1, \ldots, e_N\}$ and their signatures.
2. Construct the *distance matrix*: (in the *feature space of parameters*): $d_{ij} = d(e_i, e_j)$, $e_i, e_j \in E$.

Clustering algorithm

1. Start from N elements $E = \{e_1, \ldots, e_N\}$ and their signatures.
2. Construct the *distance matrix*: (in the *feature space of parameters*): $d_{ij} = d(e_i, e_j)$, $e_i, e_j \in E$.
3. Construct a *locally scaled affinity matrix* $\hat{A} \in \mathbb{R}^{N \times N}$:

$$\hat{A}_{ij} = \exp\left(-\frac{d_{ij}^2}{\sigma_i \sigma_j}\right) \tag{1}$$

where σ_l is a *local scaling parameter* (Zelnik) (distance of element e_i to its R-th closest neighbor).

Clustering algorithm

1. Start from N elements $E = \{e_1, \ldots, e_N\}$ and their signatures.
2. Construct the *distance matrix*: (in the *feature space of parameters*): $d_{ij} = d(e_i, e_j)$, $e_i, e_j \in E$.
3. Construct a *locally scaled affinity matrix* $\hat{A} \in \mathbb{R}^{N \times N}$:

$$\hat{A}_{ij} = \exp\left(-\frac{d_{ij}^2}{\sigma_i \sigma_j}\right) \tag{1}$$

   where σ_l is a *local scaling parameter* (Zelnik) (distance of element e_i to its R-th closest neighbor).
4. Normalize $\hat{A}$ with $D_{ii} = \sum_{j=1}^{N} \hat{A}_{ij}$ obtaining the *normalized locally scaled affinity matrix* $L = D^{-1/2} A D^{-1/2}$

Clustering algorithm

5. For N_C=min,max number of clusters:

Clustering algorithm

5. For N_C=min,max number of clusters:
   (i) Find the N_C largest eigenvectors $x_1, \ldots, x_{N_C}$ of L and form the matrix $X = [x_1, \ldots, x_{N_C}] \in \mathbb{R}^{N \times N_C}$.

Clustering algorithm

5. For N_C=min,max number of clusters:
   (i) Find the N_C largest eigenvectors $x_1, \ldots, x_{N_C}$ of L and form the matrix $X = [x_1, \ldots, x_{N_C}] \in \mathbb{R}^{N \times N_C}$.
   (ii) Re-normalize the rows of X so that they have unitary length, obtaining the matrix $Y \in \mathbb{R}^{N \times N_C}$ as $Y_{ij} = X_{ij} / \left(\sum_j X_{ij}^2 \right)^{1/2}$

Clustering algorithm

5. For N_C=min,max number of clusters:
   (i) Find the N_C largest eigenvectors $x_1, \ldots, x_{N_C}$ of L and form the matrix $X = [x_1, \ldots, x_{N_C}] \in \mathbb{R}^{N \times N_C}$.
   (ii) Re-normalize the rows of X so that they have unitary length, obtaining the matrix $Y \in \mathbb{R}^{N \times N_C}$ as $Y_{ij} = X_{ij} / \left(\sum_j X_{ij}^2 \right)^{1/2}$
   (iii) Treat each row of Y as a point in $\mathbb{R}^{N_C}$ and cluster them into N_C clusters via K-means algorithm.

Clustering algorithm

5. For N_C=min,max number of clusters:
   (i) Find the N_C largest eigenvectors $x_1, \ldots, x_{N_C}$ of L and form the matrix $X = [x_1, \ldots, x_{N_C}] \in \mathbb{R}^{N \times N_C}$.
   (ii) Re-normalize the rows of X so that they have unitary length, obtaining the matrix $Y \in \mathbb{R}^{N \times N_C}$ as $Y_{ij} = X_{ij} / \left(\sum_j X_{ij}^2 \right)^{1/2}$
   (iii) Treat each row of Y as a point in $\mathbb{R}^{N_C}$ and cluster them into N_C clusters via K-means algorithm.
   (iv) Assign the original element e_i to cluster k iff row i of Y was assigned to cluster k in the previous step.

Clustering algorithm

5. For N_C=min,max number of clusters:
   (i) Find the N_C largest eigenvectors $x_1, \dots, x_{N_C}$ of L and form the matrix $X = [x_1, \dots, x_{N_C}] \in \mathbb{R}^{N \times N_C}$.
   (ii) Re-normalize the rows of X so that they have unitary length, obtaining the matrix $Y \in \mathbb{R}^{N \times N_C}$ as $Y_{ij} = X_{ij} / \left(\sum_j X_{ij}^2 \right)^{1/2}$
   (iii) Treat each row of Y as a point in $\mathbb{R}^{N_C}$ and cluster them into N_C clusters via K-means algorithm.
   (iv) Assign the original element e_i to cluster k iff row i of Y was assigned to cluster k in the previous step.
   (v) Obtain *optimality score*, for this number of clusters N_C, based on the **silhouette coefficient**(Rousseeuw), a confidence indicator on the membership of an element to the cluster it was assigned.

Clustering algorithm

5. For N_C=min,max number of clusters:
   (i) Find the N_C largest eigenvectors $x_1, \ldots, x_{N_C}$ of L and form the matrix $X = [x_1, \ldots, x_{N_C}] \in \mathbb{R}^{N \times N_C}$.
   (ii) Re-normalize the rows of X so that they have unitary length, obtaining the matrix $Y \in \mathbb{R}^{N \times N_C}$ as $Y_{ij} = X_{ij} / \left(\sum_j X_{ij}^2\right)^{1/2}$
   (iii) Treat each row of Y as a point in $\mathbb{R}^{N_C}$ and cluster them into N_C clusters via K-means algorithm.
   (iv) Assign the original element e_i to cluster k iff row i of Y was assigned to cluster k in the previous step.
   (v) Obtain *optimality score*, for this number of clusters N_C, based on the **silhouette coefficient**(Rousseeuw), a confidence indicator on the membership of an element to the cluster it was assigned.
6. Determine the optimum number of clusters minimizing the optimality score.

Feature space of parameters

Consists of seven parameters:

- $\{\hat{S}, \hat{C}\}$,*feature center* of $\mathcal{P}(S, C)$.
- λ, stretching parameter.
- $\{d_l^S, d_u^S, d_l^C, d_u^C\}$, *feature lower/upper distances* of $\mathcal{P}(S, C)$.

Distance matrix is obtained as the Euclidean distance of points in this feature space of parameters.

Feature space of parameters

The *feature center*, $\hat{x}$, of a pdf, $f(x)$, is defined as:

$$\hat{x} \equiv \begin{cases} \bar{x} - d_l\sqrt{1 - \left(\frac{d_l}{d_u}\right)^2} & \text{if } d_l < d_u \\ \bar{x} + d_u\sqrt{1 - \left(\frac{d_u}{d_l}\right)^2} & \text{if } d_l > d_u \end{cases}$$

where $\bar{x}$ is the *mean* or *expected value* of X, $\bar{x} \equiv \int xfdx$.
The *lower* and *upper distances* d_l, d_u, are defined by:

$$d_l \equiv \sqrt{\frac{\int_{x\leq\bar{x}} (\bar{x} - x)^2 \, fdx}{\int_{x\leq\bar{x}} fdx}} \quad , \qquad d_u \equiv \sqrt{\frac{\int_{x\geq\bar{x}} (\bar{x} - x)^2 \, fdx}{\int_{x\geq\bar{x}} fdx}}$$

The *feature center* accounts for the asymmetry of $f(x)$.

Feature space of parameters

Example: $f(x) = x^2 \exp\left(-\sqrt{x}\right) / \int_0^\infty \xi^2 \exp\left(-\sqrt{\xi}\right) d\xi$

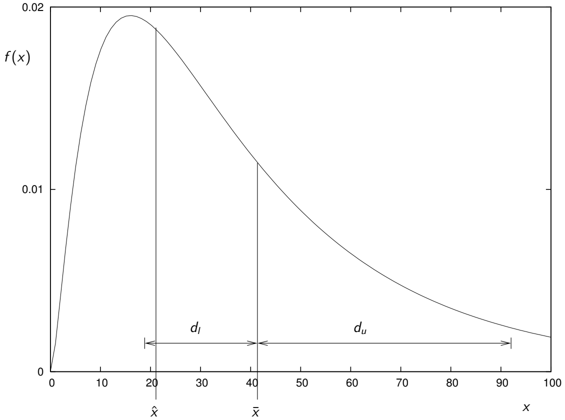

Visualization space

Based on the *feature space*, it is intended to provide a graphical representation of the distribution of individual structures.

The utilization of *glyphs*, scaling and coloring allows more than three dimensions to be represented in the *visualization space*.

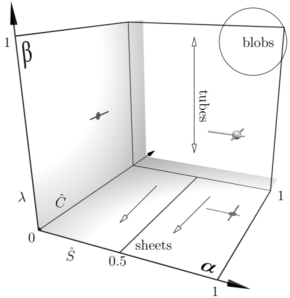

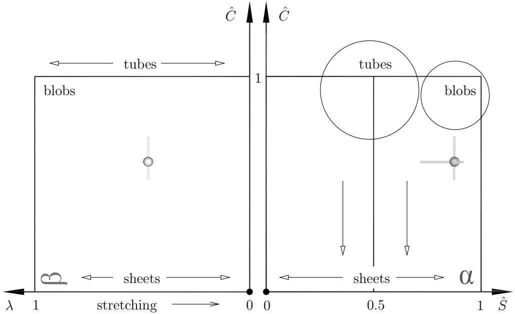

Application to virtual world of structures

Applies the characterization and classification steps to a set of nearly 200 modeled structures of different sizes and shapes.

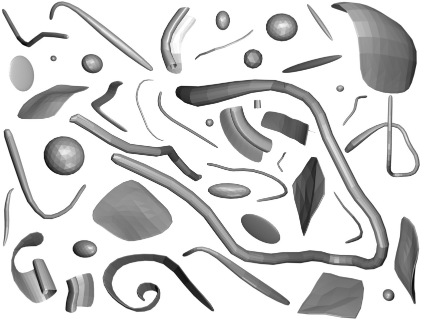

Application to virtual world of structures

Applies the characterization and classification steps to a set of nearly 200 modeled structures of different sizes and shapes.

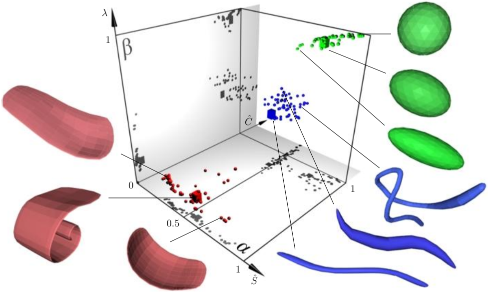

Three main groups are automatically educed (blob, tube, sheet-like) assigning each element to the correct group.

Application to virtual world of structures

Applies the characterization and classification steps to a set of nearly 200 modeled structures of different sizes and shapes.

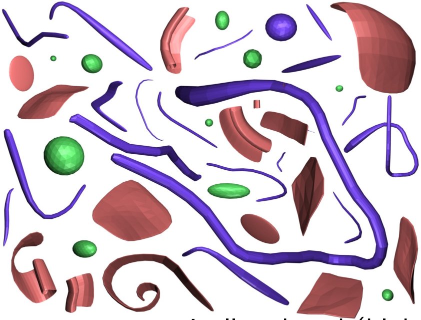

Three main groups are automatically educed (blob, tube, sheet-like) assigning each element to the correct group.

Numerical data base (O'Gorman)

- DNS with 512^3 grid points in a periodic cube $2\pi^3$.

Numerical data base (O'Gorman)

- DNS with 512^3 grid points in a periodic cube $2\pi^3$.
- The incompressible Navier-Stokes equations for the velocity field and the advection-diffusion equation for the passive scalar solved by Fourier-Galerkin pseudo-spectral method.

Numerical data base (O'Gorman)

- DNS with 512^3 grid points in a periodic cube $2\pi^3$.
- The incompressible Navier-Stokes equations for the velocity field and the advection-diffusion equation for the passive scalar solved by Fourier-Galerkin pseudo-spectral method.
- Velocity field forced at large scales, becoming statistically stationary in time.

Numerical data base (O'Gorman)

- DNS with 512^3 grid points in a periodic cube $2\pi^3$.
- The incompressible Navier-Stokes equations for the velocity field and the advection-diffusion equation for the passive scalar solved by Fourier-Galerkin pseudo-spectral method.
- Velocity field forced at large scales, becoming statistically stationary in time.
- Mean scalar gradient imposed so that the scalar fluctuation field became also statistically stationary in time.

Numerical data base (O'Gorman)

- DNS with 512^3 grid points in a periodic cube $2\pi^3$.
- The incompressible Navier-Stokes equations for the velocity field and the advection-diffusion equation for the passive scalar solved by Fourier-Galerkin pseudo-spectral method.
- Velocity field forced at large scales, becoming statistically stationary in time.
- Mean scalar gradient imposed so that the scalar fluctuation field became also statistically stationary in time.
- Scalar fluctuation statistically homogeneous.

Numerical data base (O'Gorman)

- DNS with 512^3 grid points in a periodic cube $2\pi^3$.
- The incompressible Navier-Stokes equations for the velocity field and the advection-diffusion equation for the passive scalar solved by Fourier-Galerkin pseudo-spectral method.
- Velocity field forced at large scales, becoming statistically stationary in time.
- Mean scalar gradient imposed so that the scalar fluctuation field became also statistically stationary in time.
- Scalar fluctuation statistically homogeneous.
- Reynolds number based on the integral length scale is 1901.

Numerical data base (O'Gorman)

- DNS with 512^3 grid points in a periodic cube $2\pi^3$.
- The incompressible Navier-Stokes equations for the velocity field and the advection-diffusion equation for the passive scalar solved by Fourier-Galerkin pseudo-spectral method.
- Velocity field forced at large scales, becoming statistically stationary in time.
- Mean scalar gradient imposed so that the scalar fluctuation field became also statistically stationary in time.
- Scalar fluctuation statistically homogeneous.
- Reynolds number based on the integral length scale is 1901.
- Taylor Reynolds number is $Re_T = 265$.

Numerical data base (O'Gorman)

- DNS with 512^3 grid points in a periodic cube $2\pi^3$.
- The incompressible Navier-Stokes equations for the velocity field and the advection-diffusion equation for the passive scalar solved by Fourier-Galerkin pseudo-spectral method.
- Velocity field forced at large scales, becoming statistically stationary in time.
- Mean scalar gradient imposed so that the scalar fluctuation field became also statistically stationary in time.
- Scalar fluctuation statistically homogeneous.
- Reynolds number based on the integral length scale is 1901.
- Taylor Reynolds number is $Re_T = 265$.
- Schmidt number of the simulation is 0.7.

Numerical data base (O'Gorman)

- DNS with 512^3 grid points in a periodic cube $2\pi^3$.
- The incompressible Navier-Stokes equations for the velocity field and the advection-diffusion equation for the passive scalar solved by Fourier-Galerkin pseudo-spectral method.
- Velocity field forced at large scales, becoming statistically stationary in time.
- Mean scalar gradient imposed so that the scalar fluctuation field became also statistically stationary in time.
- Scalar fluctuation statistically homogeneous.
- Reynolds number based on the integral length scale is 1901.
- Taylor Reynolds number is $Re_T = 265$.
- Schmidt number of the simulation is 0.7.
- $k_{max}\eta = 1.05$.

Multiscale diagnosis

512^3 points $\Rightarrow$ 7 scales available in curvelet domain:

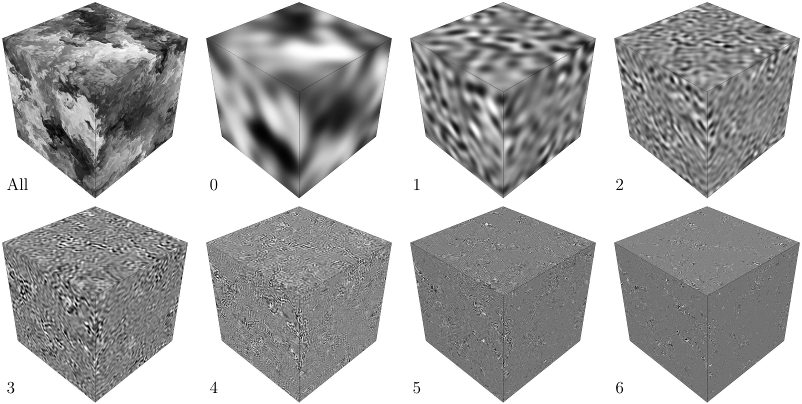

Plane cuts of cube faces

Multiscale diagnosis

512^3 points $\Rightarrow$ 7 scales available in curvelet domain:

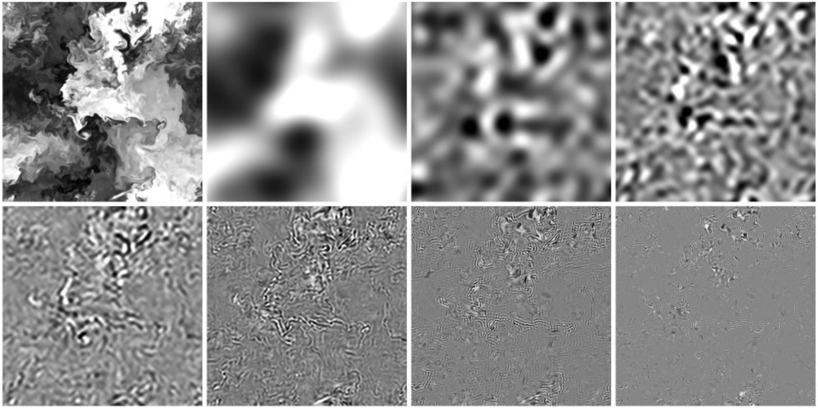

Plane cuts normal to z axis.

Multiscale diagnosis

512^3 points $\Rightarrow$ 7 scales available in curvelet domain:

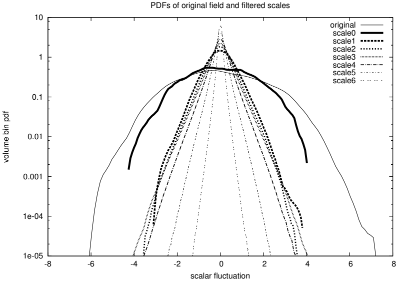

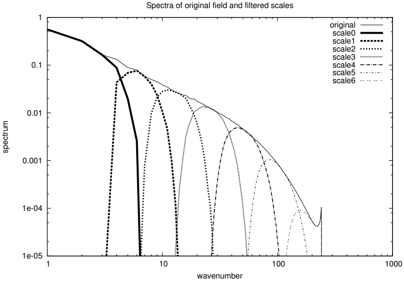

Volume data pdfs and spectra of passive scalar fluctuation fields.

Multiscale diagnosis

512^3 points $\Rightarrow$ 7 scales available in curvelet domain:

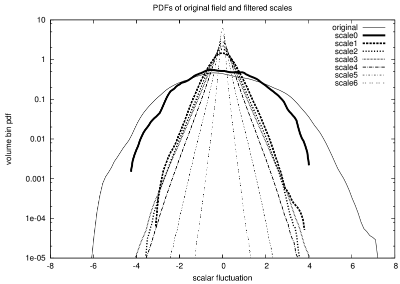

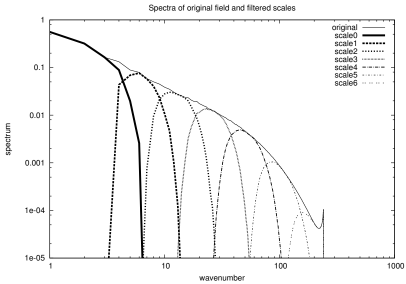

Volume data pdfs and spectra of passive scalar fluctuation fields.

Pdfs of scales 1, 2, 3 (inertial range) almost collapse, getting narrower for dissipation scales (4, 5, 6).

Multiscale diagnosis

An equivalent decomposition is done for the velocity field.

Multiscale diagnosis

An equivalent decomposition is done for the velocity field.

Define characteristic squared integral velocities, $\overline{u_i^2}$, and integral length scales, L_i and L_i', for each scale i as:

$$\overline{u_i^2} = \frac{2}{3}\int_0^\infty E_i(k)dk,\ L_i = \frac{\pi}{2\overline{u^2}}\int_0^\infty \frac{E_i(k)}{k}dk,\ L_i' = \frac{\pi}{2\overline{u_i^2}}\int_0^\infty \frac{E_i(k)}{k}dk$$

where $E_i(k)$ is the energy spectrum associated to scale i

Multiscale diagnosis

An equivalent decomposition is done for the velocity field.

Define characteristic squared integral velocities, $\overline{u_i^2}$, and integral length scales, L_i and L_i', for each scale i as:

$$\overline{u_i^2} = \frac{2}{3}\int_0^\infty E_i(k)dk,\; L_i = \frac{\pi}{2\overline{u^2}}\int_0^\infty \frac{E_i(k)}{k}dk,\; L_i' = \frac{\pi}{2\overline{u_i^2}}\int_0^\infty \frac{E_i(k)}{k}dk$$

where $E_i(k)$ is the energy spectrum associated to scale i

From the properties of the filtering in curvelet domain:

$$E(k) = \sum_i E_i(k), \qquad \overline{u^2} = \sum_i \overline{u_i^2}$$

Multiscale diagnosis

An equivalent decomposition is done for the velocity field.

scale	$\overline{u_i^2}/\overline{u^2}$	L_i/η †	L_i'/η
original	1.000	249.6	249.6
0	0.591	226.9	383.8
1	0.155	14.68	96.1
2	0.113	5.235	46.2
3	0.085	1.927	22.8
4	0.044	0.519	11.9
5	0.011	0.070	6.3
6	0.001	0.004	3.3

† $\eta \equiv$ Kolmogorov length-scale

Iso-contours

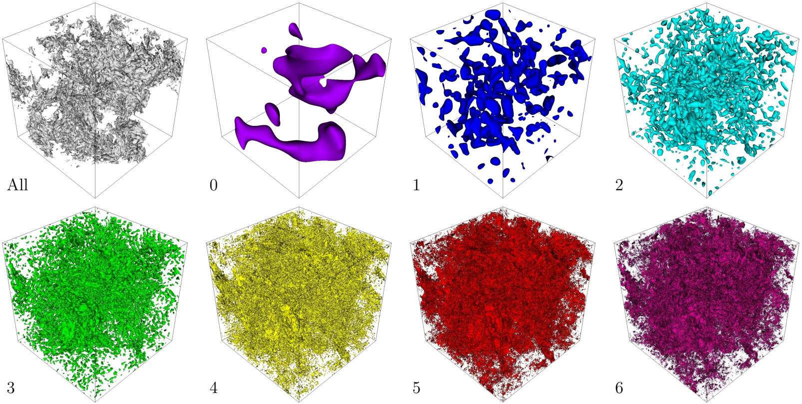

Iso-contours of original field and filtered scales.

Iso-contours

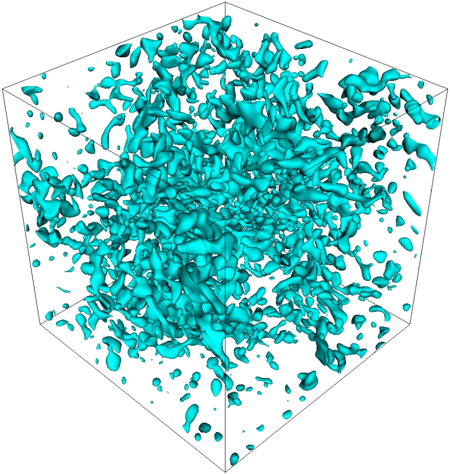

Iso-contours filtered scale 2.

Iso-contours

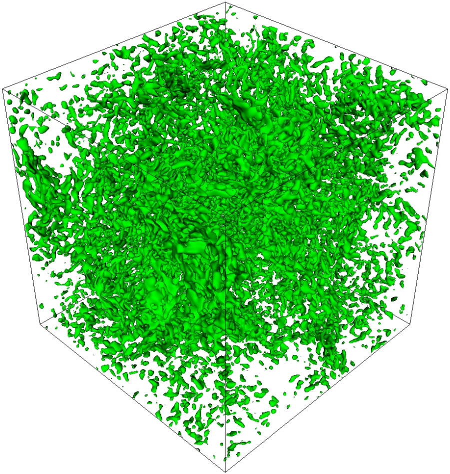

Iso-contours filtered scale 3.

Iso-contours

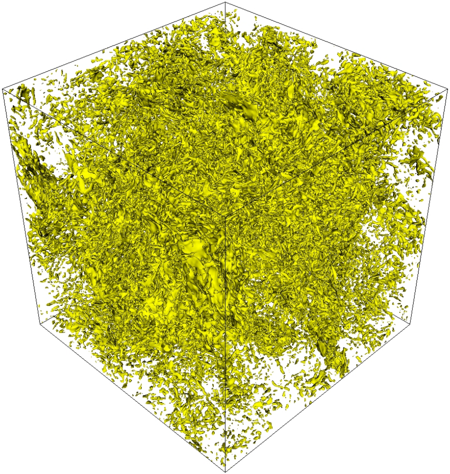

Iso-contours filtered scale 4.

Iso-contours

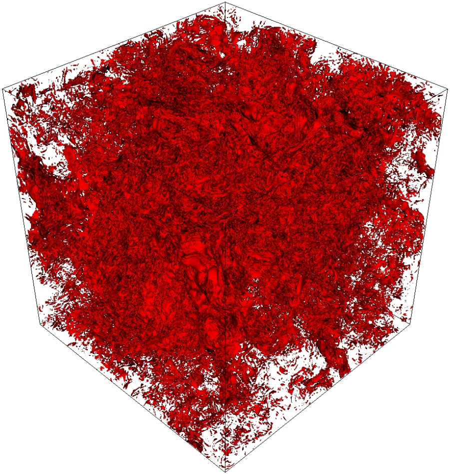

Iso-contours filtered scale 5.

Individual structures - Visualization space

Individual structures corresponding to scales 1-5 are characterized.

Scales 0 (largest) and 6 (smallest) are not included:

- scale 0 $\Rightarrow$ dependent on the boundary conditions.
- scale 6 $\Rightarrow$ ignored to avoid lack of spatial resolution and aliasing effects.

First, individual structures are represented in a *visualization space* by spheres with:

- center $= \{\hat{S}, \hat{C}, \lambda\}$.
- color $\Rightarrow$ filtered scale number in curvelet space.
- radius $=$ area of the surface, in a log-normalized scale.

Individual structures - Visualization space

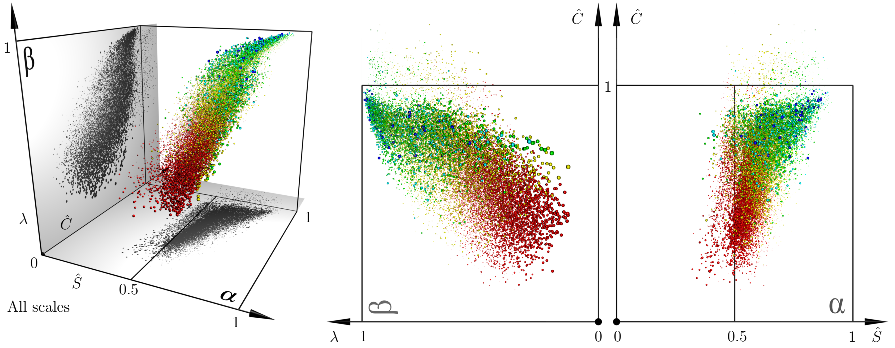

- center $= \{\hat{S}, \hat{C}, \lambda\}$.
- color $\Rightarrow$ filtered scale number in curvelet space.
- diameter $=$ area of the surface, in a log-normalized scale.

Individual structures - Visualization space

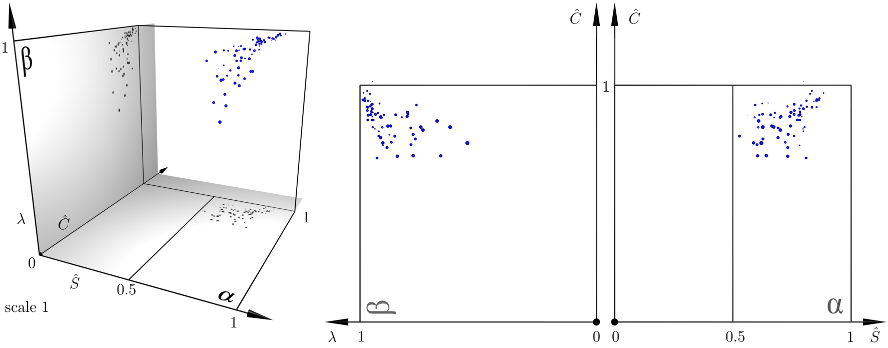

- center $= \{\hat{S}, \hat{C}, \lambda\}$.
- color $\Rightarrow$ filtered scale number in curvelet space.
- diameter $=$ area of the surface, in a log-normalized scale.

Individual structures - Visualization space

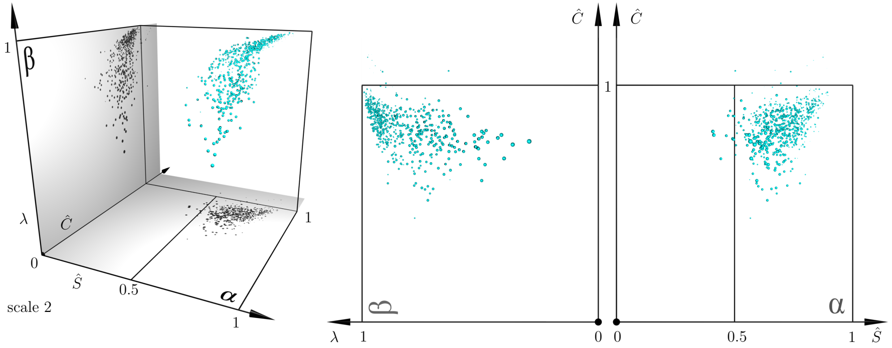

- center $= \{\hat{S}, \hat{C}, \lambda\}$.
- color $\Rightarrow$ filtered scale number in curvelet space.
- diameter $=$ area of the surface, in a log-normalized scale.

Individual structures - Visualization space

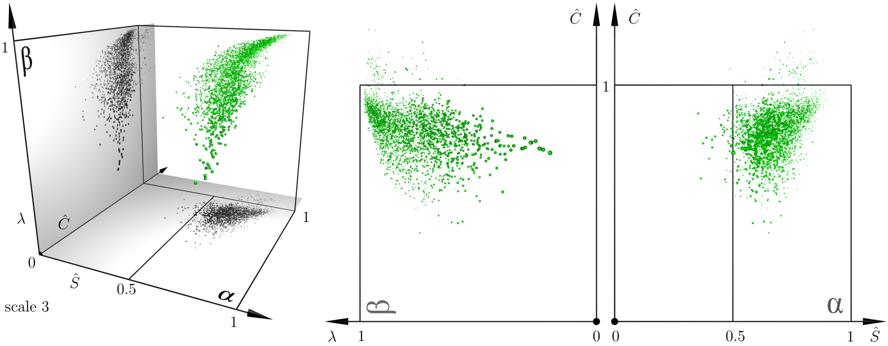

- center $= \{\hat{S}, \hat{C}, \lambda\}$.
- color $\Rightarrow$ filtered scale number in curvelet space.
- diameter $=$ area of the surface, in a log-normalized scale.

Individual structures - Visualization space

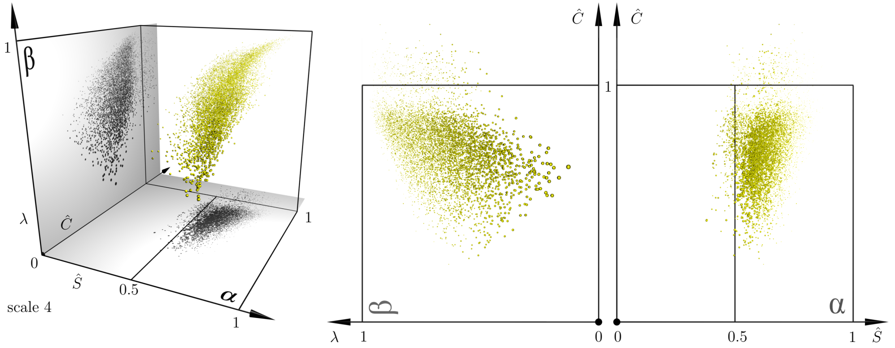

- center $= \{\hat{S}, \hat{C}, \lambda\}$.
- color $\Rightarrow$ filtered scale number in curvelet space.
- diameter $=$ area of the surface, in a log-normalized scale.

Individual structures - Visualization space

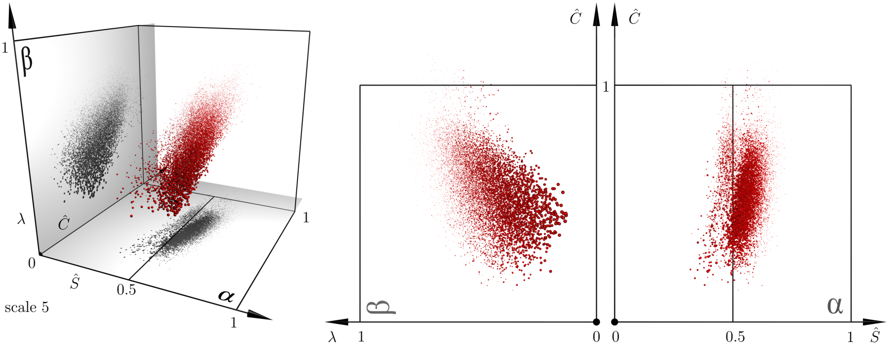

- center $= \{\hat{S}, \hat{C}, \lambda\}$.
- color $\Rightarrow$ filtered scale number in curvelet space.
- diameter $=$ area of the surface, in a log-normalized scale.

Individual structures - Visualization space

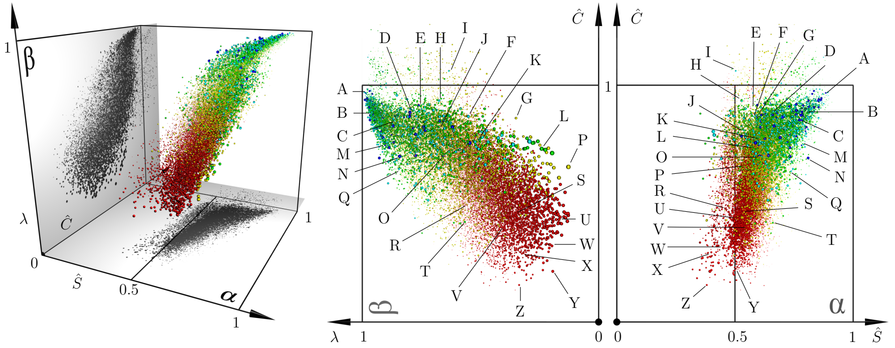

Representative points:

- $A, B, C \rightarrow$ blob-like.
- $D, E, F \rightarrow$ transition to tube-like with low/moderate stretching.

Individual structures - Visualization space

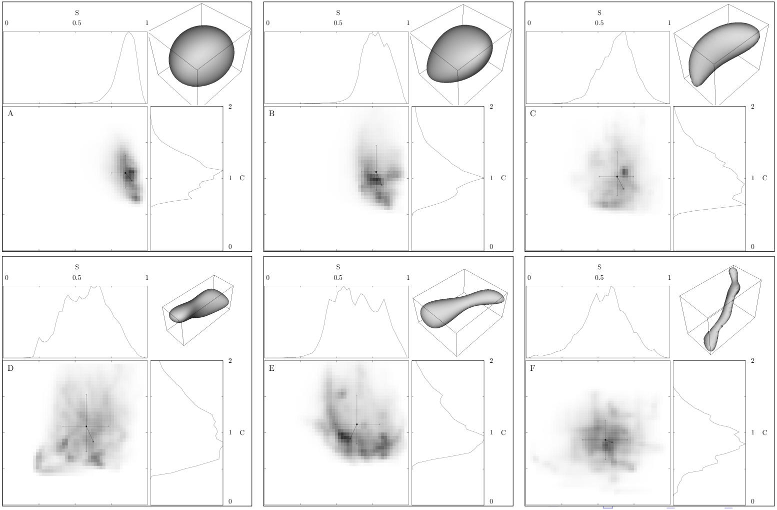

Individual structures - Visualization space

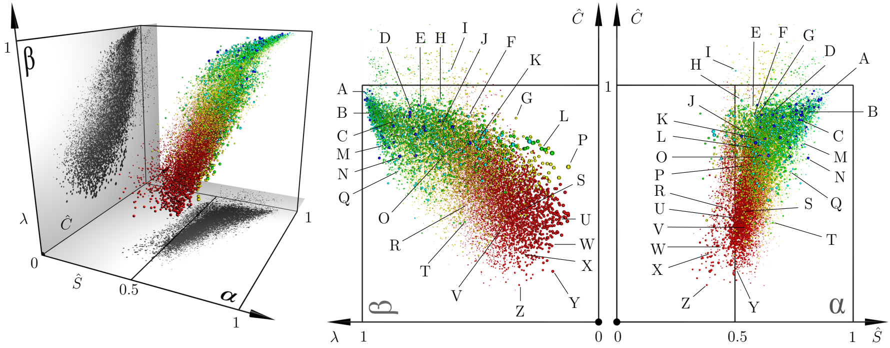

Representative points:

- $H, I, K, L \rightarrow$ tube-like with increasing stretching/complexity.
- $J, M \rightarrow$ patches with smaller curvedness.

Individual structures - Visualization space

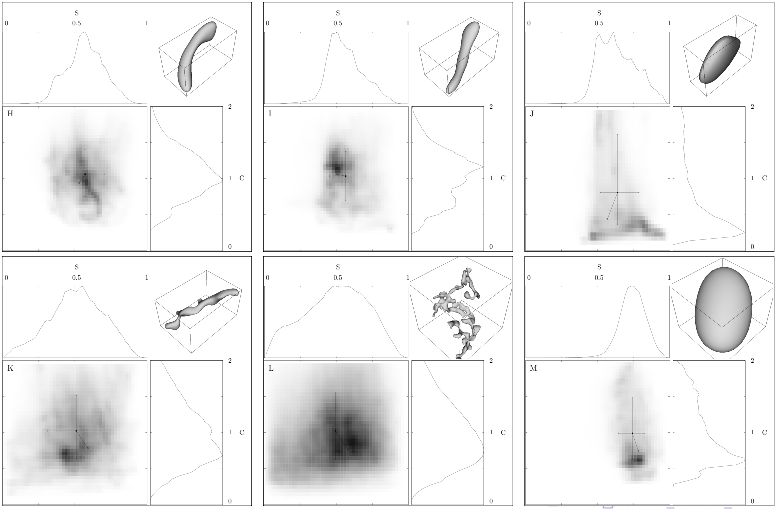

Individual structures - Visualization space

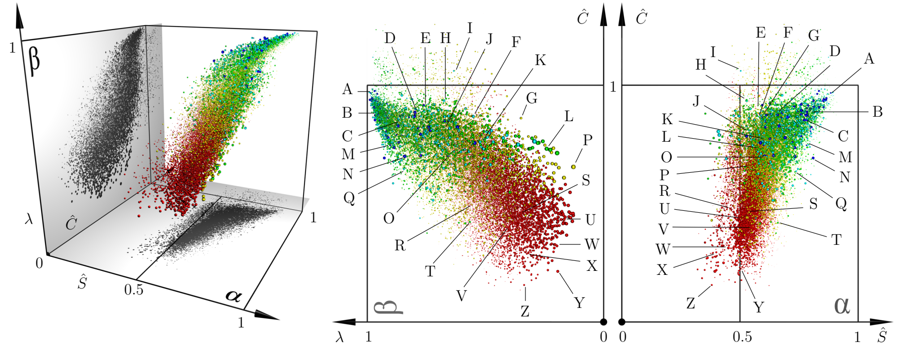

Representative points:

- $N, O, P \rightarrow$ lower curvedness with increasing stretching/complexity.
- $Q, R, S \rightarrow$ decreasing curvedness $\rightarrow$ sheet-like.

Individual structures - Visualization space

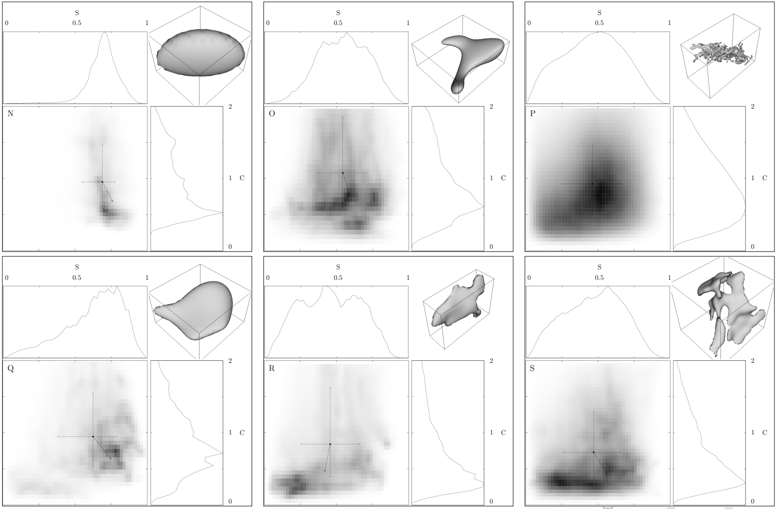

Individual structures - Visualization space

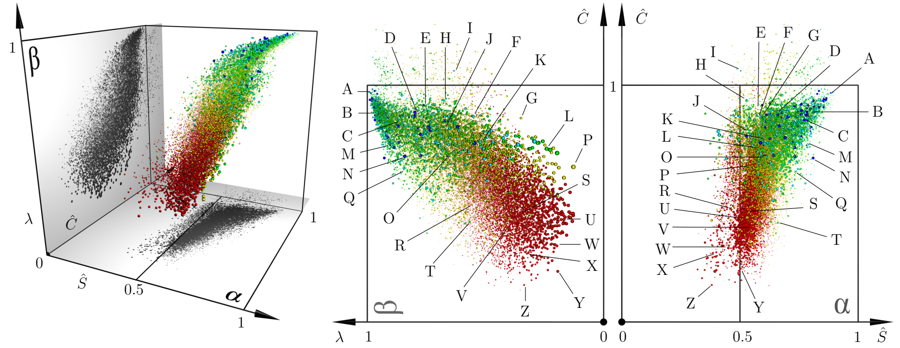

Representative points:

- $T - Z \rightarrow$ sheet-like.

Individual structures - Visualization space

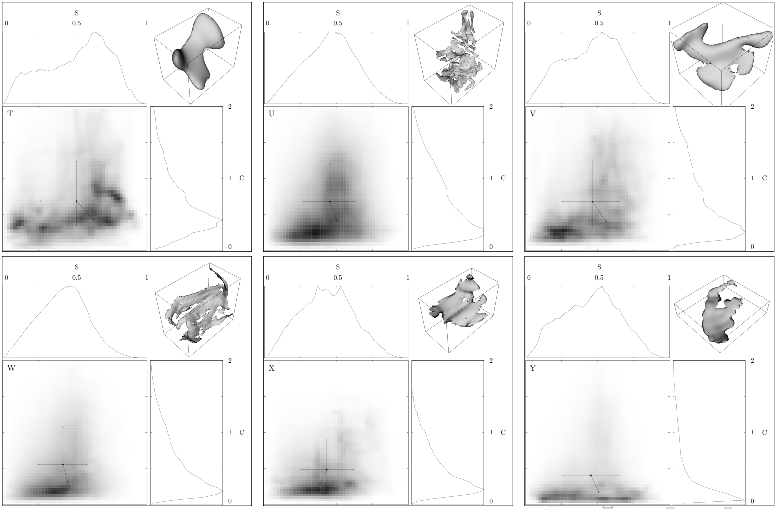

Classification via clustering

The *feature space* of parameters used for clustering includes $\{\hat{S}, \hat{C}, \lambda, d_u^S, d_l^S, d_u^C, d_l^C\}$

The clustering results are represented in a *visualization space*, where each sphere represents a structure.

- center $= \{\hat{S}, \hat{C}, \lambda\}$.
- color $\Rightarrow$ cluster ID.
- radius $\Rightarrow$ silhouette coefficient, SC, (degree of membership to the assigned cluster).
- bars $\Rightarrow d_l^S, d_u^S, d_l^C, d_u^C$, scaled by SC.

Classification via clustering

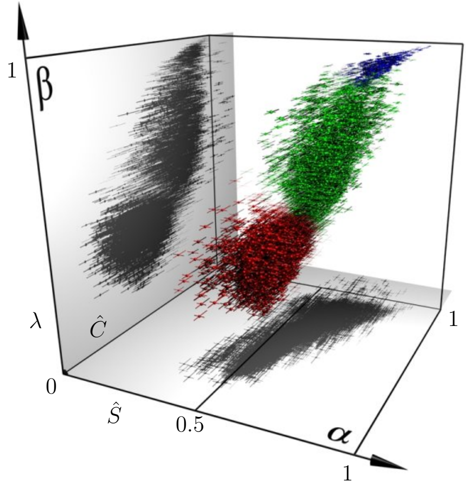

Glyphs (sphere+bars):

- center $= \{\hat{S}, \hat{C}, \lambda\}$.
- color $\Rightarrow$ cluster ID.
- radius $\Rightarrow$ SC.
- bars $\Rightarrow$ $d_l^S, d_u^S, d_l^C, d_u^C$.

Numerical data base (Horiuti)

- DNS with $256^3, 512^3$ and $1024^{3\dagger}$ grid points in a periodic cube.

$^\dagger 1024^3$ case currently under analysis. Only results for 256^3 and 512^3 shown.

Numerical data base (Horiuti)

- DNS with $256^3, 512^3$ and $1024^{3\dagger}$ grid points in a periodic cube.
- Homogeneous isotropic turbulence.

$^\dagger 1024^3$ case currently under analysis. Only results for 256^3 and 512^3 shown.

Numerical data base (Horiuti)

- DNS with $256^3, 512^3$ and $1024^{3\dagger}$ grid points in a periodic cube.
- Homogeneous isotropic turbulence.
- Taylor Reynolds numbers: $Re_T = 77.2, 76.87, 77.43$.

$^\dagger 1024^3$ case currently under analysis. Only results for 256^3 and 512^3 shown.

Numerical data base (Horiuti)

- DNS with $256^3, 512^3$ and $1024^{3\dagger}$ grid points in a periodic cube.
- Homogeneous isotropic turbulence.
- Taylor Reynolds numbers: $Re_T = 77.2, 76.87, 77.43$.
- $k_{max}\eta = 1.02, 2.05, 4.09$.

$^\dagger 1024^3$ case currently under analysis. Only results for 256^3 and 512^3 shown.

Numerical data base (Horiuti)

- DNS with $256^3, 512^3$ and $1024^{3\dagger}$ grid points in a periodic cube.
- Homogeneous isotropic turbulence.
- Taylor Reynolds numbers: $Re_T = 77.2, 76.87, 77.43$.
- $k_{max}\eta = 1.02, 2.05, 4.09$.
- Same initial conditions in the three cases.

$^\dagger 1024^3$ case currently under analysis. Only results for 256^3 and 512^3 shown.

Numerical data base (Horiuti)

- DNS with $256^3, 512^3$ and $1024^{3\dagger}$ grid points in a periodic cube.
- Homogeneous isotropic turbulence.
- Taylor Reynolds numbers: $Re_T = 77.2, 76.87, 77.43$.
- $k_{max}\eta = 1.02, 2.05, 4.09$.
- Same initial conditions in the three cases.
- Purpose: Study effect of increasing resolution on the geometry of structures.

$^\dagger 1024^3$ case currently under analysis. Only results for 256^3 and 512^3 shown.

Numerical data base (Horiuti)

- DNS with $256^3, 512^3$ and $1024^{3\dagger}$ grid points in a periodic cube.
- Homogeneous isotropic turbulence.
- Taylor Reynolds numbers: $Re_T = 77.2, 76.87, 77.43$.
- $k_{max}\eta = 1.02, 2.05, 4.09$.
- Same initial conditions in the three cases.
- Purpose: Study effect of increasing resolution on the geometry of structures.
- Scalar field of study: square of the vorticity.

$^\dagger 1024^3$ case currently under analysis. Only results for 256^3 and 512^3 shown.

Plane cut comparison - 256^3 vs 512^3 vs 1024^3

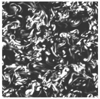

256^3

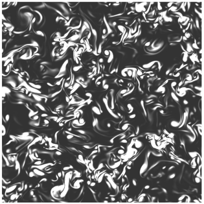

512^3

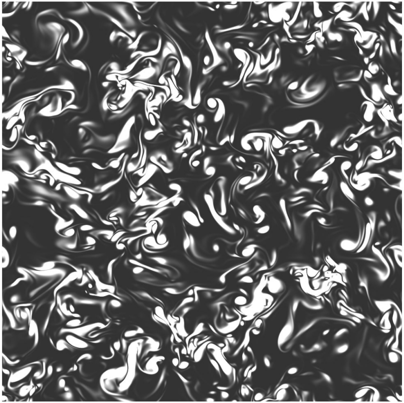

1024^3

Plane cut comparison - 256^3 vs 512^3 vs 1024^3

256^3

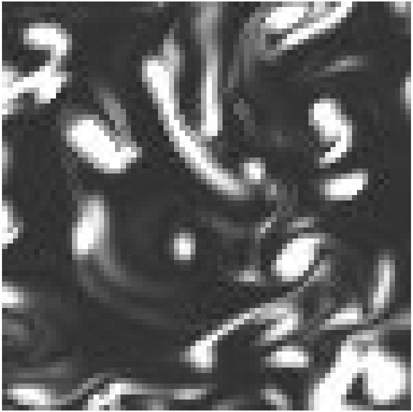

zoom

Plane cut comparison - 256^3 vs 512^3 vs 1024^3

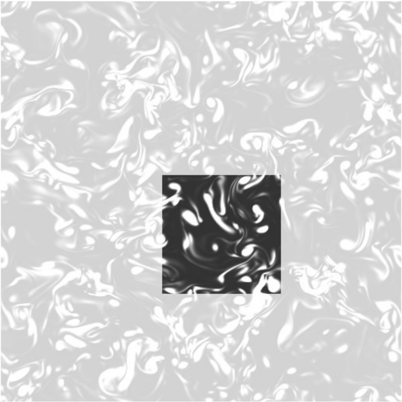

512^3

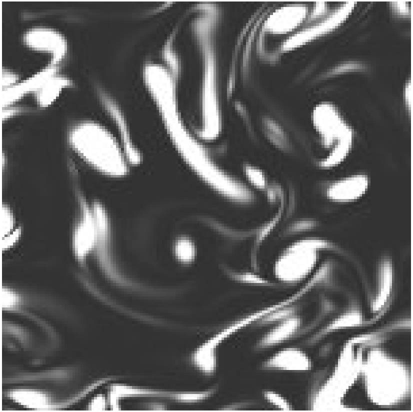

zoom

Plane cut comparison - 256^3 vs 512^3 vs 1024^3

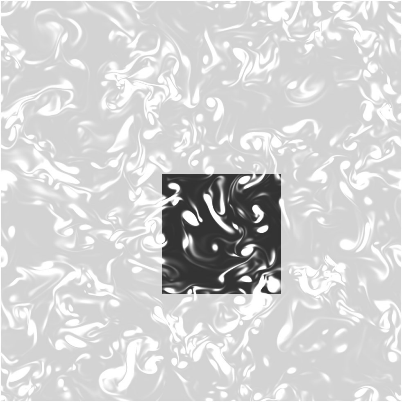

1024^3

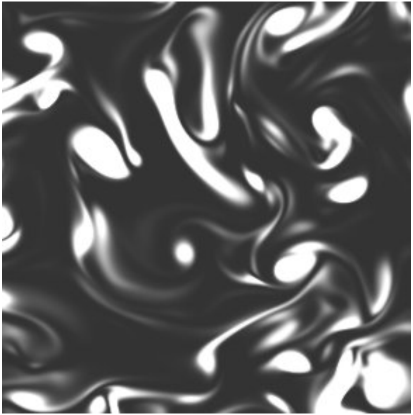

zoom

Multiscale diagnosis

256^3 points $\Rightarrow$ 6 scales available in curvelet domain:

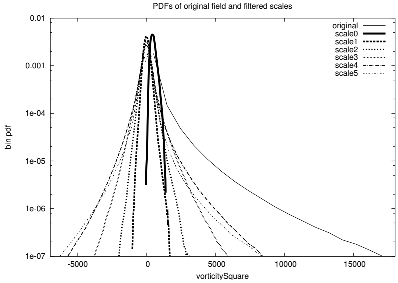

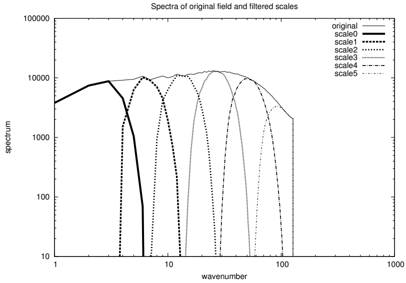

Volume data pdfs and spectra of ω^2. 256^3 run.

Multiscale diagnosis

512^3 points $\Rightarrow$ 7 scales available in curvelet domain:

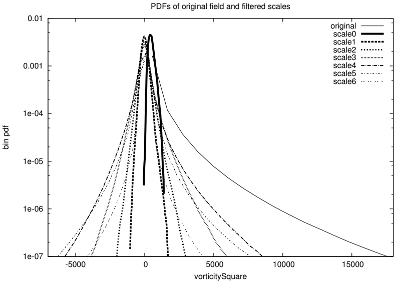

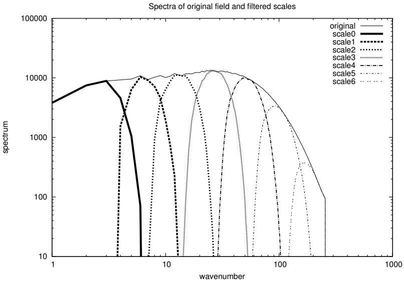

Volume data pdfs and spectra of ω^2. 512^3 run.

Multiscale diagnosis

512^3 points $\Rightarrow$ 7 scales available in curvelet domain:

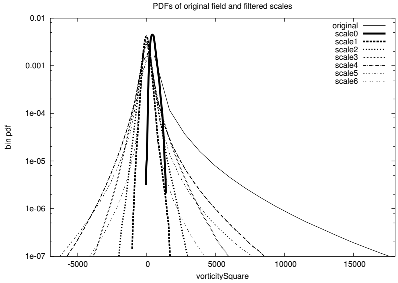

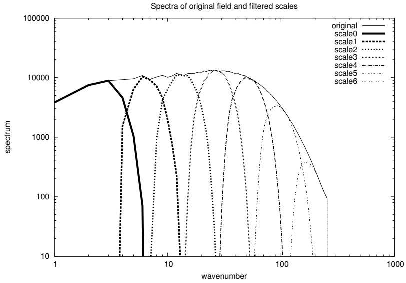

Volume data pdfs and spectra of ω^2. 512^3 run.

Pdfs of scales 1-4 get wider, and 4-6 get narrower.

Isocontours - 256^3 vs 512^3

scale 1

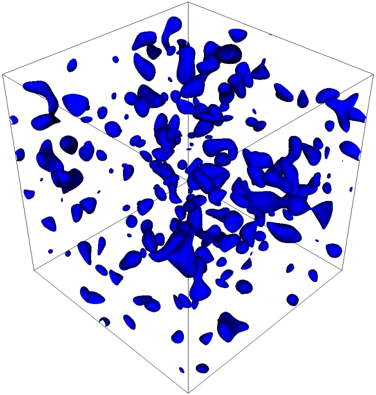

256^3

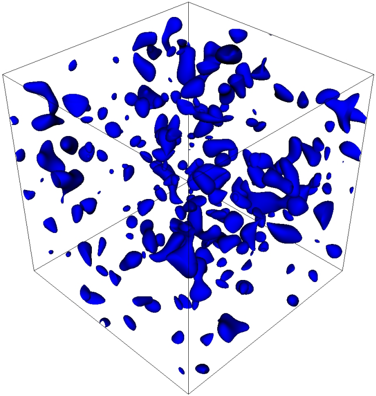

512^3

Isocontours - 256^3 vs 512^3

scale 2

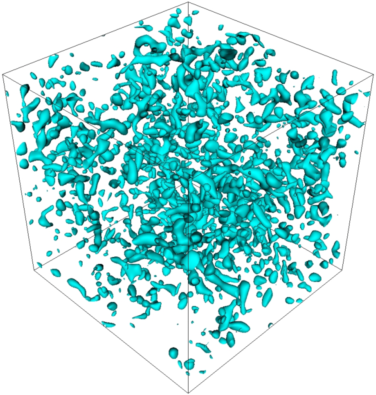

256^3

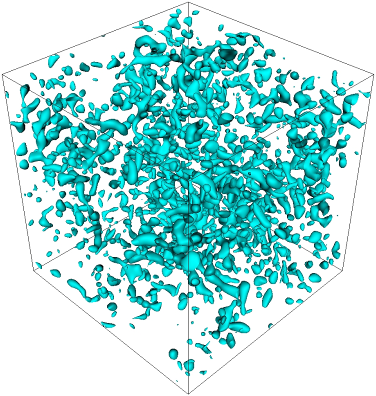

512^3

Isocontours - 256^3 vs 512^3

scale 3

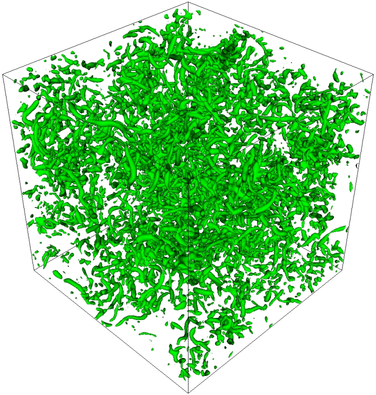

256^3

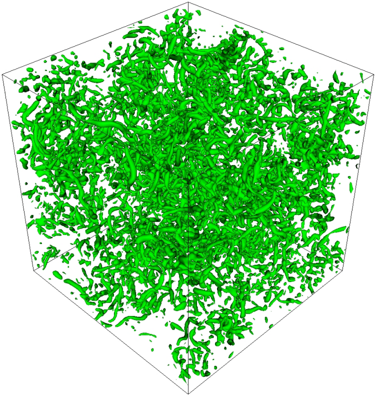

512^3

Isocontours - 256^3 vs 512^3

scale 4

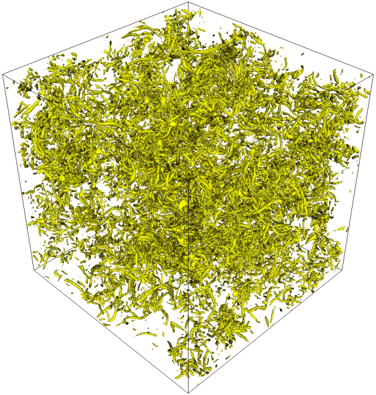

256^3

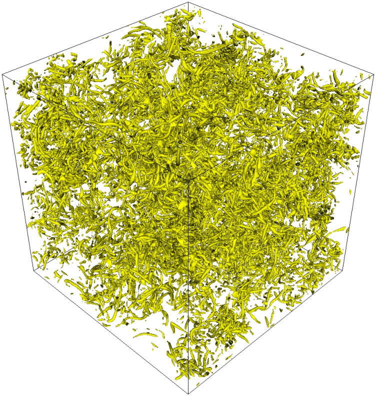

512^3

Isocontours - 256^3 vs 512^3

scale 5

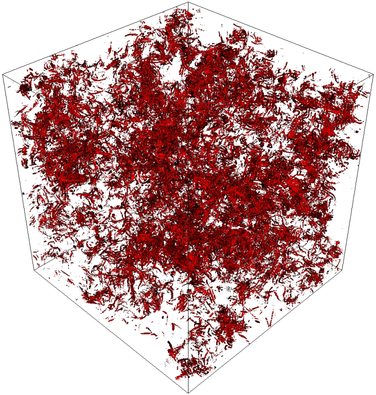

256^3 (tube-like still predominant)

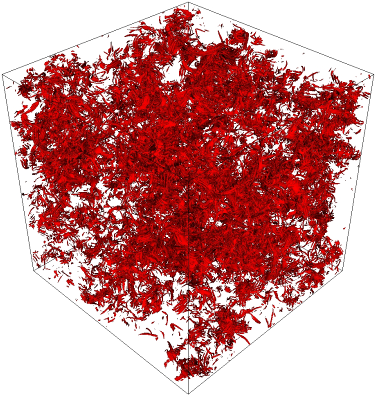

512^3 (more sheet-like)

Isocontours - 256^3 vs 512^3

scale 6

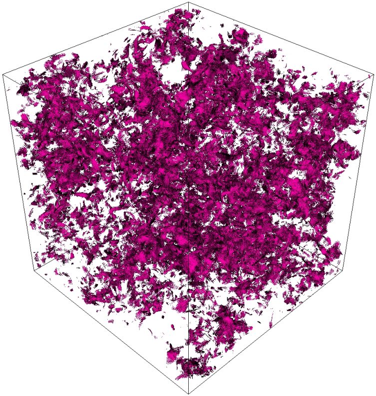

512^3

Isocontours - 512^3 - zoom scales 4 and 5

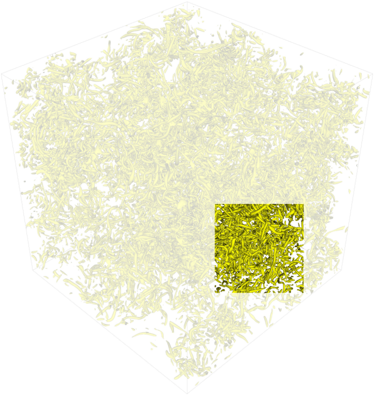

scale 4

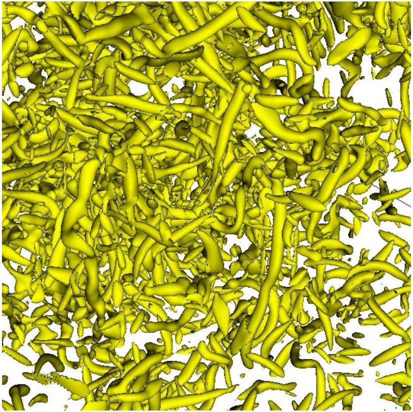

zoom

Isocontours - 512^3 - zoom scales 4 and 5

scale 5

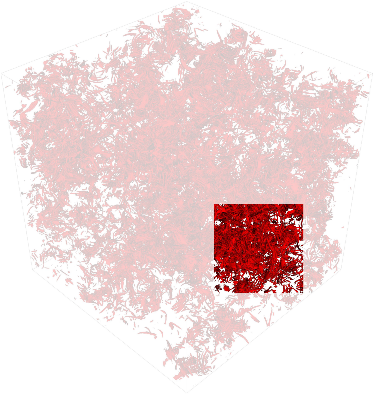

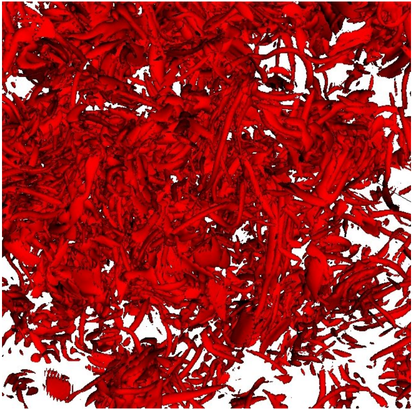

zoom

Individual structures - visualization space - 256^3 vs 512^3

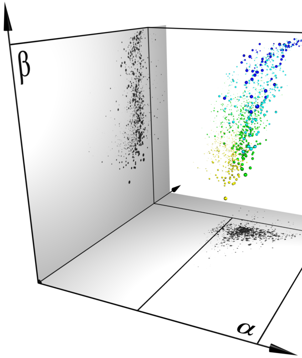

256^3 - scales 1-4

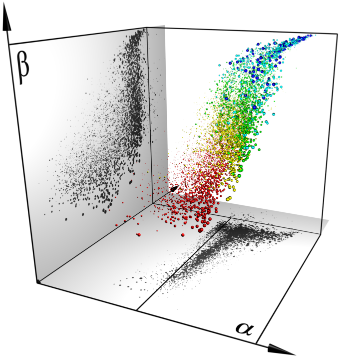

512^3 - scales 1-5

Individual structures - visualization space - 256^3 vs 512^3

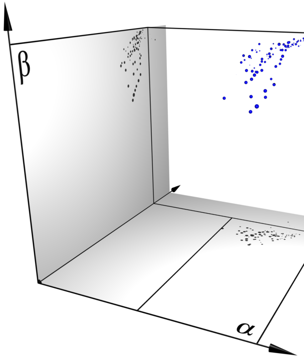

256^3 - scales 1

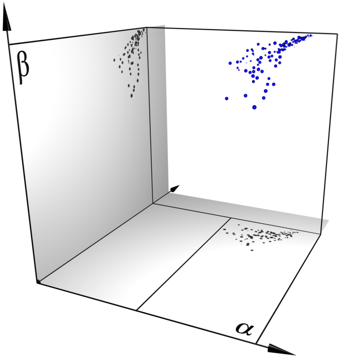

512^3 - scales 1

Individual structures - visualization space - 256^3 vs 512^3

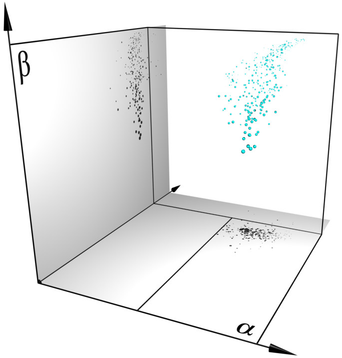

256^3 - scale 2

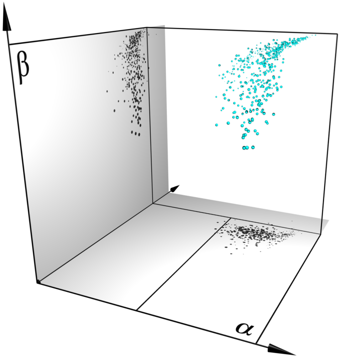

512^3 - scale 2

Individual structures - visualization space - 256^3 vs 512^3

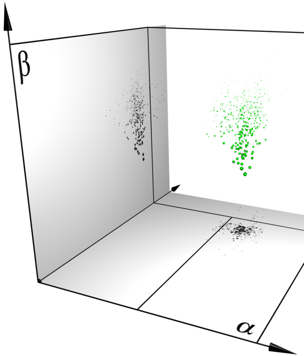

256^3 - scale 3

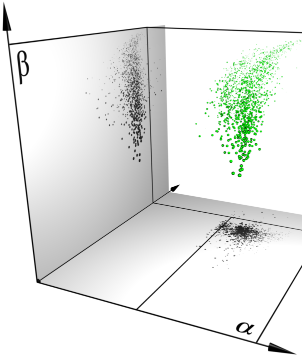

512^3 - scale 3

Individual structures - visualization space - 256^3 vs 512^3

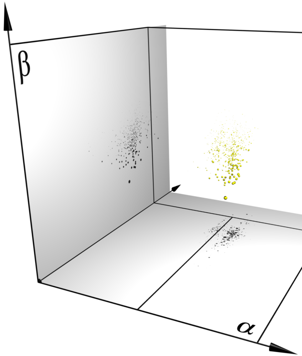

256^3 - scale 4

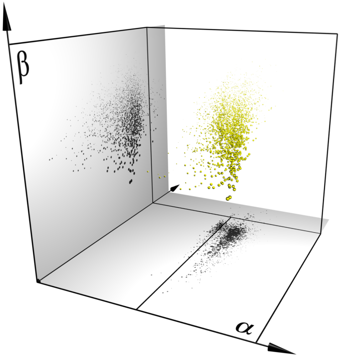

512^3 - scale 4

Individual structures - visualization space - 256^3 vs 512^3

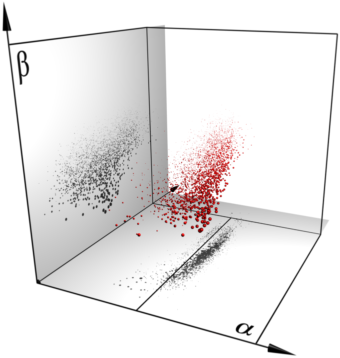

512^3 - scale 5

Individual structures - rolling geometry - scale 5 - 512^3

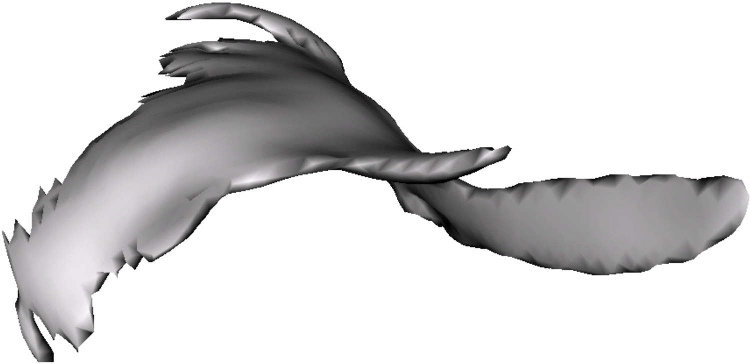

Individual structures - rolling geometry - scale 5 - 512^3

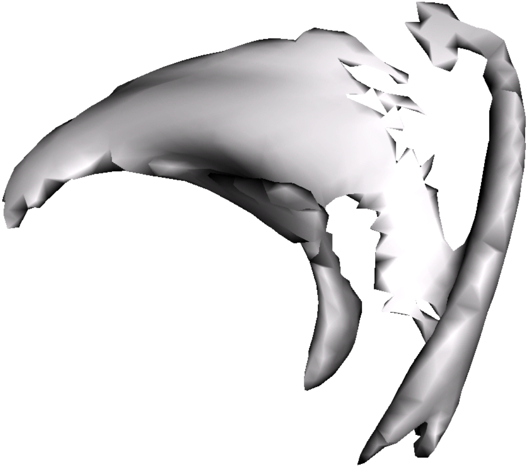

Individual structures - rolling geometry - scale 5 - 512^3

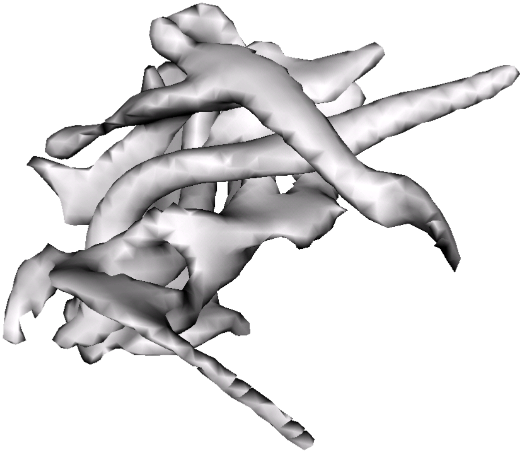

Individual structures - rolling geometry - scale 5 - 512^3

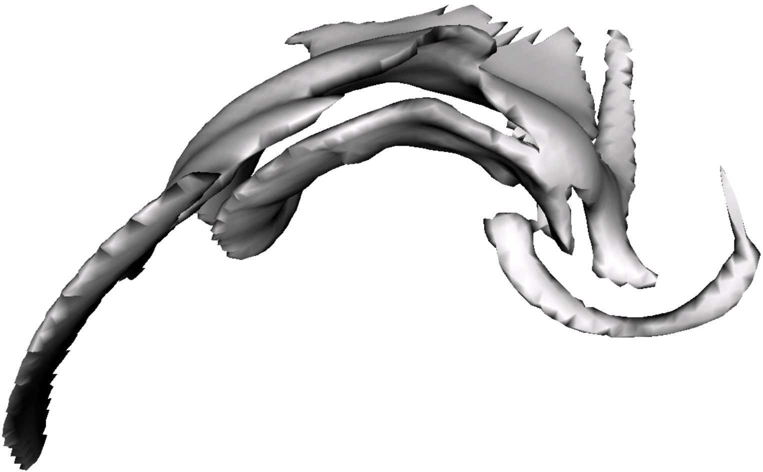

Conclusions

New methodology for the identification of structures in turbulence:

- multi-scale, non-local, geometry-based
- three main steps: extraction, characterization, classification

Conclusions

New methodology for the identification of structures in turbulence:

- multi-scale, non-local, geometry-based
- three main steps: extraction, characterization, classification

Application to passive scalar fluctuation field (512^3):

- smaller scales present narrower volume pdfs (overlapping in the inertial range)
- geometry of individual structures evolves from blob/tube-like with low to moderate stretching in the inertial range towards tube/sheet-like with high stretching in the dissipation range.
- smooth transition of geometry $\rightarrow$ difficult clustering (not clearly distinct groups $\rightarrow$ other clustering techniques can be applied: density-based, fuzzy c-means)

Conclusions

New methodology for the identification of structures in turbulence:

- multi-scale, non-local, geometry-based.
- three main steps: extraction, characterization, classification.

Application to **vorticity square** field $(256^3, 512^3)$:

- 256^3, $k_{max}\eta \approx 1 \Rightarrow$ blob to tube-like structures for smaller scales.
- 512^3, $k_{max}\eta \approx 2 \Rightarrow$ blob to tube to sheet-like structures for smaller scales.
- increasing resolution shows, for the same Reynolds number, the appearance of sheet structures with rolling geometry at the smallest scales.